ISSN 1070-3284, Russian Journal of Coordination Chemistry, 2017, Vol. 43, No. 5, pp. 320–330. © Pleiades Publishing, Ltd., 2017.

Synthesis, Characterization, and Biological Activity of Cd(II) and Mn(II) Coordination Polymers Based on Pyridine-2,6-Dicarboxylic Acid[1]

S. E. H. Etaiw[a], M. M. El-Bendary[a, b, *], and H. Abdelazim[a]

[a] *Chemistry Department, Faculty of Science, Tanta University, Tanta, Egypt*

[b] *Chemistry Department, Faculty of Science, University of Jeddah, Jeddah, Saudi Arabia*

**e-mail: elbendary1983@yahoo.com*

Received March 9, 2016

Abstract—The coordination polymers (CPs) {[Cd(Pydc)$(H_2O)_3$] · $PydcH_2$} (**I**) and [Mn(Pydc)$(H_2O)_3$] · $PydcH_2$} (**II**) were obtained by the reaction of $CdSO_4 \cdot 5H_2O$ or $MnCl_2 \cdot 4H_2O$ with pyridine-2,6-dicarboxylic acid ($PydcH_2$). The structures of the CPs **I** and **II** were characterized by IR, UV-Vis, TGA, and X-ray single crystal analysis (CIF files CCDC nos. 1417757 (**I**), 1417758 (**II**)). The network structures of **I** and **II** are constructed by an infinite number of discrete binuclear molecules and free $PydcH_2$. The structures of the CPs **I** and **II** connected by the extensive H-bonds and π–π stacking, forming a 3D-network. The CPs **I** and **II** were screened to test their antimicrobial activities against different species of bacteria and fungi.

Keywords: Cd(II) and Mn(II), coordination polymers, pyridine-2,6-dicarboxylic acid, spectra, antimicrobial activities

DOI: 10.1134/S1070328417050013

INTRODUCTION

The design and synthesis of novel coordination polymers (CPs) have attracted great attention in the fields of inorganic and coordination chemistry [1]. The self-assembly process driven by coordination chemistry has generated many fascinating structures from discrete molecular cages to three-dimensional (3D) porous frameworks [2, 3]. Because of their tunable and porous nature, CPs show desired properties in applications such as gas storage, catalysis, molecular sensing and biological and antitumor activity [4–11].

The selection of appropriate organic ligands in the design and synthesis of CPs is a key step. The carboxylate ligands are versatile ligands, which can provide abundant coordination modes and generate various interesting structures and functional properties [12–14]. On the one hand, the nitrogen-containing ligands have been proven the powerful precursor for the construction of diverse dimensional structures and topologies [15–17]. Furthermore, the combination of multicarboxylate anions with the N-donor auxiliary ligands provides a good strategy for the construction of novel topological CPs. On the other hand, multicarboxylate organic ligands feature excellent structural contributors for their various coordination modes. Therefore, pyridine-based ligands, as a family of N-donor ligands, play important roles in the construction of CPs [1–20]. For instances, bridging ligands of polycarboxylate and polyamine or organic ligands containing nitrogen and oxygen hybrid atom were often used. Recently, several novel structural coordination polymers containing the derivative of pyrazinecarboxylate or pyridinecarboxylate have been obtained [21–24]. Complexation of metal ions by pyridine carboxylic acids reveals an interesting tendency: the chelating ability of the heteronitrogen seems to depend on its position relative to the carboxylic group. Biological activities of complexes have been well documented and derivatives have been successfully screened for various actions; some have been used in commercial fungicides [25]. The Co(II), Ni(II), Cu(II), and Zn(II) complexes are biologically active and they exhibit enhanced activities as compared to their parent ligands [26]. It is well knowen that pyridine-2,6-dicarboxylic acid ($PydcH_2$) is present in large amounts in bacterial spores [27, 28]. It is the main component of bacterial spores, in which it forms a metal complex with divalent metal ions, especially with the calcium ion [29]. So, here we report the synthesis and structural characterization of the coordination polymers {[Cd(Pydc)$(H_2O)_3$] · $PydcH_2$} (**I**) and {[Mn(Pydc)$(H_2O)_3$] · $PydcH_2$} (**II**). Furthermore, the spectral characteristics of **I** and **II** have been also investigated. In addition, the antimicrobial activity has been investigated.

[1] The article is published in the original.

EXPERIMENTAL

Materials and physical measurements. All chemicals and solvents used in this study were of analytical grade supplied by Aldrich or Merck and used as received. Microanalyses (C, H, N) were carried out with a Perkin Elmer 2400 automatic elemental analyzer. IR spectra were recorded on Perkin Elmer 1430 Ratio Recording Infrared Spectrophotometer as KBr discs. Thermogravimetric (TG) analysis was carried out on a Shimadzu AT 50 thermal analyzer (under N_2 atmosphere). Electronic absorption spectra as solid matrices were measured on Shimadzu (UV-310l PC) spectrometer. Fluorescent spectra as solid matrices were measured with a Perkin Elmer (LS 50 B) spectrometer ($\lambda_{ex} = 300$ nm).

Synthesis of I and II. A solution of 74 mg (0.25 mmol) of $CdSO_4 \cdot 5H_2O$ in 20 mL H_2O or 49 mg (0.25 mmol) of $MnCl_2 \cdot 4H_2O$ was added under gentle stirring to a solution of 55 mg (0.3 mmol) of $PydcH_2$ as a ligand in 20 mL CH_3CN-H_2O (1 : 1) at room temperature. A white precipitate was formed then after filtration, the filtrate was kept at room temperature. After three weeks, white crystals were obtained that were filtrated, washed with small quantity of cold H_2O, and overnight dried.

For $C_{14}H_{14}N_2O_{11}Cd$ (**I**)			
anal. calcd., %:	C, 33.72;	H, 2.83;	N, 5.62.
Found, %:	C, 33.61;	H, 2.76;	N, 5.65.
For $C_{14}H_{14}N_2O_{11}Mn$ (**II**)			
anal. calcd., %:	C, 38.11;	H, 3.20;	N, 6.35.
Found, %:	C, 38.13;	H, 3.21;	N, 6.38.

X-ray structure determination. Structural measurements for **I** and **II** were performed on a Kappa CCd Enraf Nonius FR 90 four circle goniometer with graphite monochromatic MoK_α radiation (λ(MoK_α) = 0.71073 Å) at 298 ± 2 K. The structures were solved using direct–methods and all of the non-hydrogen atoms were located from the initial solution or from subsequent electron density difference maps during the initial stages of the refinement. After locating all of the non-hydrogen atoms in each structure the models were refined against F^2, first using isotropic and finally using anisotropic thermal displacement parameters. The positions of the hydrogen atoms were then calculated and refined isotropically, and the final cycle of refinements was performed. Crystallographic data for the CPs **I** and **II** are summarized in Table 1. Selected bond distances and bond angles are given in Table 2. Geometric parametrs of hydrogen bond in **I** and **II** are listed in Table 3.

Supplementary material for structures has been deposited with the Cambridge Crystallographic Data Centre (CCDC 1417757 (**I**), 1417758 (**II**); deposit@ccdc.cam.ac.uk or http://www.ccdc.cam.ac.uk/conts/retrieving.html).

Antimicrobial assessment. *Staphylococcus aureus* and *Escherchia coli* are chosen as the bacterial microorganisms while the fungal microorganisms used are *Aspergillus flavus*, *Candida albicans*, and *Asperigllus niger* to test the antimicrobial activity of the CPs **I** and **II.** Nutrient agar was used for growing bacterial cultures. On the other hand, Sabouraud dextrose agar was used for the growth of *C. albicans* and Cazpek's dox agar was used for the growth of *A. flavus* and *A. niger.* The tested compounds were solved in DMSO. A 0.5 mL spores or cell suspension were prepared and counted, then mixed with 9.5 mL of the corresponding sterilized melted media, and left to solidify at room temperature. Wells are made in seeded agar plate with different organisms under investigation by cork borer with diameter 8 mm and each one was filled with 5 mg of the CPs **I** and **II**. All the plates were incubated at proper temperature and time and then the inhibition zone diameters were measured. Tetracycline was used as antibacterial control and Amphotericin B was used as antifungal control for comparing the results with their inhibition zones.

RESULTS AND DISCUSSION

$PydcH_2$ is a versatile multidentate N- and O-donor ligand which can be considered a crucial factor for the construction of the coordination polymer architectures of **I** and **II**. In fact, our goal was the preparation of complexes of Cd(II) or Mn(II) and $PydcH_2$ with an auxillary ligand; mainly cyanide or thiocyanate ions. In all cases, we obtained the CPs **I** and **II** which are auxillary ligand free compounds. So, the CPs **I** and **II** were obtained by the conventional solution method by treating metal ion of Cd(II) or Mn(II) and $PydcH_2$ in H_2O–acetonitrile solution. The crystal structures of the CPs **I** and **II** will be compared with those briefly reported in [23, 24]. The asymmetric units of the CPs **I** and **II** consist of one crystallographically independent Cd(II) and Mn(II) atoms, two organic ligands one coordinated to the metal ion as pyridine-2,6-dicarboxylate (Pydc) and one is free as $PydcH_2$ and three coordinated water molecules. In the CPs **I** and **II**, the Pydc ligand adopted one kind of coordination mode with Cd(II) or Mn(II) metal centres. In this aspect, nitrogen and two oxygen atoms are involved in chelation to form two five membered rings (Fig. 1). Two asymmetric units form a repeat unit containing two metal cations coordinated to two Pydc ligand and three H_2O molecules in addition to one free $PydcH_2$ (Fig. 2). The charge neutrality is achieved by the deprotonated carboxylate group of the Pydc ligand.

In the extended structures of the CPs **I** and **II**, there are two crystallographically identical Cd(II) or Mn(II) atoms. Each Cd(II) or Mn(II) atom is surrounded by seven atoms, four of them are coming from

Table 1. Crystallographic data and structure refinements for **I** and **II**

Parameter	Value	
	I	**II**
Formula weight	498.669	441.207
Crystal size, mm	0.27 × 0.27 × 0.20	0.25 × 0.25 × 0.22
Crystal system	Monoclinic	Monoclinic
Space group	$P2_1/c$	$P2_1/c$
a, Å	9.1985(2)	9.1802(2)
b, Å	14.7170(4)	14.6200(3)
c, Å	12.2722(3)	12.2075 3)
β, deg	97.589(2)	97.4688(12)
V, Å^3	1646.79(7)	1624.52(6)
Z	4	4
ρ_{calcd}, mg cm^{-3}	2.011	1.804
$F(000)$	992	604
$\mu(MoK_\alpha)$, mm^{-1}	1.39	0.88
θ Range for data collection, deg	2–60	2–60
Index range of hkl	$-14 \le h \le 14$, $0 \le k \le 22$, $-18 \le l \le 18$	$-14 \le h \le 14$, $0 \le k \le 23$, $-14 \le l \le 14$
Collected reflection	6305	7217
Independent reflections	6593	6994
Reflection with $I > 2\sigma(I)$	3818	4726
R_{int}	(0.045)	(0.045)
Parameters refined	253	263
Data/restraints/parameters	3818/0/253	7217/0/263
Goodness-of-fit on F^2	1.009	1.565
Final R indices ($I > 2\sigma(I)$	0.039/0.129	0.052/0.103
R indices(all data)	0.068/0.132	0.068/0.103
$\Delta\rho_{max}$, $\Delta\rho_{min}$, e Å^{-3}	1.11/–2.03	0.94/–0.78

two Pydc ligands. Here, in CP **I** two basal coordination sites are occupied by one nitrogen and one of the oxygen atom of Pydc ligand (Cd(1)–O(10) 2.476(2) and Cd(1)–N(5) 2.322(2) Å) and other two basal coordination sites are occupied by the two μ_2-oxygen atoms (O(3)) from two Pydc ligands (Cd(1)–O(3) 2.398(2) and Cd(1)–O(3)^i 2.37582(2) Å). The fifth basal coordination site is occupied by one water molecule (Cd–O(9) 2.261(2) Å). The two apical coordination sites are occupied by the other two water molecules (Cd(1)–O(8) 2.432(2) and Cd(1)–O(6) 2.315(2) Å) (Table 2). The CPs **I** and **II** are isostrutural. Thus, the seven-coordinated Cd(II) or Mn(II) atoms exhibit unusual distorted pentagonal bipyramidal geometry (Fig. 2, Table 2). The basal angles of the pentagon of CP **I** are within the range 102.99°–115.82° whereas for apical angles, they equal 91.41° (O(3)Cd(1)O(6)) and 89.49° (O(6)Cd(1)O(10)). The distortion of the pentagon in the case of CP **II** is more pronounced than CP **I** where the basal angles of the pentagon are within the range 101.86°–114.97° and the apical angles equal 91.54° (O(4)Mn(1)O(5)) and 88.04° (O(2)Mn(1)O(5)). In **I**, one of the carboxylate groups functions as a bridging ligand connecting two adjacent Cd(II) centers resulting in the formation of mini cycle motif; Cd_2O_2 with Cd–Cd distance equals to 3.916 Å. Each cadmium site contains two five member chelate rings. The cadmium sites and the two Pydc ligands are in the same plane forming discrete sheet. These sheets are interconnected to the free $PydcH_2$ via H-bonds between the hydrogen atoms of the water molecules and the $PydcH_2$ ligand forming 1D chain (Fig. 3, Table 3). On the other hand, the extensive hydrogen bonds between coordinated water molecules and/or the carboxylate groups of the Pydc ligands and the free $PydcH_2$ ligands (2.480–3.028 Å) form 2D layer

Table 2. Bond lengths (Å) and bond angles (deg) of the CP **I** and **II***

Bond	*d*, Å	Bond	*d*, Å
		I	
Cd(1)–O(3)	2.398(2)	O(3)Cd(1)O(3)^{i}	69.74(7)
Cd(1)–O(3)^{i}	2.375(2)	O(3)Cd(1)N(5)	69.04(7)
Cd(1)–N(5)	2.322(2)	O(3)Cd(1)O(6)	91.42(7)
Cd(1)–O(6)	2.315(2)	O(3)Cd(1)O(8)	87.57(7)
Cd(1)–O(8)	2.432(2)	O(3)Cd(1)O(9)	150.83(7)
Cd(1)–O(9)	2.261(2)	O(3)Cd(1)O(10)	135.69(6)
Cd(1)–O(10)	2.476(2)	O(3)^{i}Cd(1)N(5)	138.76(7)
C(17)–O(10)	1.265(2)	O(6)Cd(1)O(8)	165.74(6)
C(27)–O(3)	1.262(2)	Cd(1)O(3)Cd(1)^{i}	110.26(7)
Cd(1)–Cd(1)^{i}	3.916(4)	O(3)^{i}Cd(1)O(9)	81.55(7)
		O(3)^{i}Cd(1)O(10)	153.94(7)
		Cd(1)O(3)O(6)^{i}	106.39(8)
		Cd(1)O(3)O(9)^{i}	157.42(8)
		II	
Mn(1)–O(5)	2.3148	O(5)Mn(1)O(5)^{i}	69.3501
Mn(1)–O(5)^{i}	2.3164	O(5)Mn(1)N(13)	70.3604
Mn(1)–N(13)	2.2902	O(5)Mn(1)O(4)	91.5367
Mn(1)–O(4)	2.1949	O(5)Mn(1)O(2)	88.0394
Mn(1)–O(2)	2.3107	O(5)Mn(1)O(8)	136.8044
Mn(1)–O(8)	2.4739	O(5)Mn(1)O(29)	151.6167
Mn(1)–O(29)	2.1760	O(5)^{i}Mn(1)N(13)	139.7076
C(19)–O(6)	1.241	O(5)^{i}Mn(1)O(4)	83.2710
C(19)–O(5)	1.280	Mn(1)O(5)Mn(1)^{i}	110.6499
C(22)–O(8)	1.271	Mn(1)O(5)O(5)^{i}	55.3538
C(24)–O(11)	1.289	Mn(1)O(5)N(13)	54.3855
Mn(1)–Mn(1)^{i}	3.809	Mn(1)O(5)O(6)	145.1917
		Mn(1)O(5)C(18)	84.3980

* Symmetry codes: ^{i} $-x, -y, 2-z$ (**I**); ^{i} $1-x, -y, 1-z$ (**II**).

(Fig. 4, Table 3). The 3D network structures of the CPs **I** and **II** are coordinated Pydc and the pridiyle rings of the free $PydcH_2$ (3.634–3.795 Å) (Fig. 5). Comparing the structures of the CPs **I** and **II** with the reported compounds $[Mn_2(C_7H_3NO_4)_2(H_2O)_6] \cdot 2C_7H_5NO_4$ (**III**) and $[Cd_2(C_7H_3NO_4)_2(H_2O)_6] \cdot 2C_7H_5NO_4$ (**IV**) indicate that they are isostructures [23, 24]. However, while the asymmetric units of CPs **I** and **II** are mononuclear, **III** and **IV** are centrosymmetric binuclear complexes with $Z = 2$ [23, 24]. Most of the crystal structures of the complexes of $PydcH_2$ ligand with Ti^{2+}, Ag^{2+}, Sr^{2+}, Ni^{2+}, Cu^{2+}, and Zn^{2+} indicate that the ligand is coordinated to a mononuclear metal ion and acts as a terdentate ligand, in which the central metal ion is bonded to two N and four O atoms of two ligand molecules [30–35]. But the Ti^{4+}, Fe^{2+}, and Ca^{2+} complexes are binuclear complexes [31, 36, 37]. The structures of CPs **I** and **II** are 3D networks via extensive H-bonds and π–π stacking.

The IR spectra of the CPs **I** and **II** and the free $PydcH_2$ ligand are shown in Table 4. The IR spectra of **I** and **II** show a broad absorption band in the range of 3250–3400 and 3200–3408 cm^{-1}, respectively. These bands are assigned to the stretching vibrations of O–H bonds of water molecules in **I** and **II**, respectively. The positions of these bands give an indication the existence of O–H···O hydrogen bonding between the water molecules [38, 39]. The carboxylate ion may coordinate to a metal atom in one of the unidentate, bidentate or bridging modes [40]. The band associated

Table 3. Geometric parametrs of hydrogen bonds in **I** and **II**

D–H···A	Distance, Å			Angle DHA, deg
	D–H	H···A	D···A	
		I		
C(24)–H(24)···O(4)	0.96	2.48	3.179(2)	130
C(30)–H(30)···O(22)	0.96	2.93	3.821(2)	1553
C(33)–H(33)···O(9)	0.96	2.68	3.529(7)	148
C(30)–H(30)···O(6)	0.96	3.00	3.410(7)	107
C(13)–H(13)···O(6)	0.96	2.62	3.527(5)	158
C(28)–H(28)···O(6)	0.96	3.03	3.427(8)	107
O(19)–H(19)···O(8)	0.96	2.39	2.849(7)	110
O(8)–H(8*A*)···O(11)	0.96	2.22	3.120(7)	156
O(8)–H(8*A*)···N(12)	0.96	2.34	2.943(2)	120
O(6)–H(6*A*)···O(7)	0.96	2.81	2.694(2)	73
		II		
C(14)–H(14)···O(12)	1.01	2.49	3.239(2)	127
C(20)–H(20)···O(4)	0.96	2.68	3.590(2)	158
C(26)–H(26)···O(6)	0.96	2.47	3.163(7)	129
C(17) –H(17)···O(9)	0.96	2.89	3.772(8)	154
C(16)–H(16)···O(9)	0.96	3.01	3.674(7)	127
C(16) –H(16)···O(29)	0.96	2.76	3.602(7)	146
C(16)–H(16)···O(6)	0.96	3.04	3.435(6)	106
C(14)–H(14)···O(12)	1.06	2.49	3.239(5)	127
O(2)–H(2*A*)···O(10)	0.96	2.28	2.943(2)	120
C(14)–H(14)···O(4)	1.06	3.02	3.473(7)	106
C(24)–O(11)···H(2*B*)	1.24	2.75	3.880(8)	145
C(22)–O(7)···H(4*B*)	1.24	2.52	3.703(8)	157
C(22)–O(7)···H(4*A*)	1.24	2.81	3.639(7)	123

to the antisymmetric stretching vibrational mode of carboxylate groups, $\nu_{as}(COO^-)$ appears at 1450 cm^{-1} (**I**) and 1439 cm^{-1} (**II**), together with the $\nu_s(COO^-)$ band at 1380 cm^{-1} (**I**) and 1392 cm^{-1} (**II**). The values of $\Delta(\nu_{as}(COO^-) - \nu_s(COO^-))$ indicate the presence of carboxylate group coordinated to metal ions, which is in agreement with the crystal structures of **I** and **II**. On the other hand, the stretching vibrations of the OH-carboxylate group of **I** and **II** appear at 2550 and 2555 cm^{-1}, respectively. Also strong absorptions appear at 544 and 442 cm^{-1} in the spectra of **I** and **II** which are absent in the spectrum of $PydcH_2$ corresponding to the M–O and M–N stretching vibrations. The bands at 3084 and 3052 cm^{-1} for **I** and **II** can be attributed to aromatic ν(C–H) vibrations and the strong band at 638 and 726 cm^{-1} for **I** and **II**, respectively, is attributed to γCH. The selected strong band at 1598 and 1593 cm^{-1} for **I** and **II**, respectively, can be assigned to ν(C=N) and that at 1693 and 1693 cm^{-1} can be assigned to ν(C=O) (Table 4). These bands appear at lower wavenumbers than those of the free $PydcH_2$ ligand indicating that the relevant oxygen and nitrogen of the ligand are coordinated to the metal.

TGA for the CPs **I** and **II** were carried out in the temperature range from 25 to 1000°C under N_2 gas. The DTA thermogram of **I** shows three exothermic peaks while that of **II** exhibits two exothermic peaks (Fig. 6). The first step corresponds to decomposition of the coordinated water molecules in the range of 80–110°C with weight loss of 10.6 and 12.5% (calcd. 10.8 and 12.2%), for the CPs **I** and **II**, respectively. The second and the third steps in the thermogram of the CP **I** between 115 to 415°C indicates the removal of the the free and coordinated 2,6-pyridine dicarboxylate ligands with a weight loss of 63.6% (calcd. 63.7%). On the other hand, the decomposition of the free and coordinated 2,6-pyridine dicarboxylate ligands with a weight loss of 72.5% (calcd. 72%) appears in the second step in the thermogram of the CP **II** in the temperature range of 110 to 410°C. The molecular weight of the residue obtained after complete thermolysis of

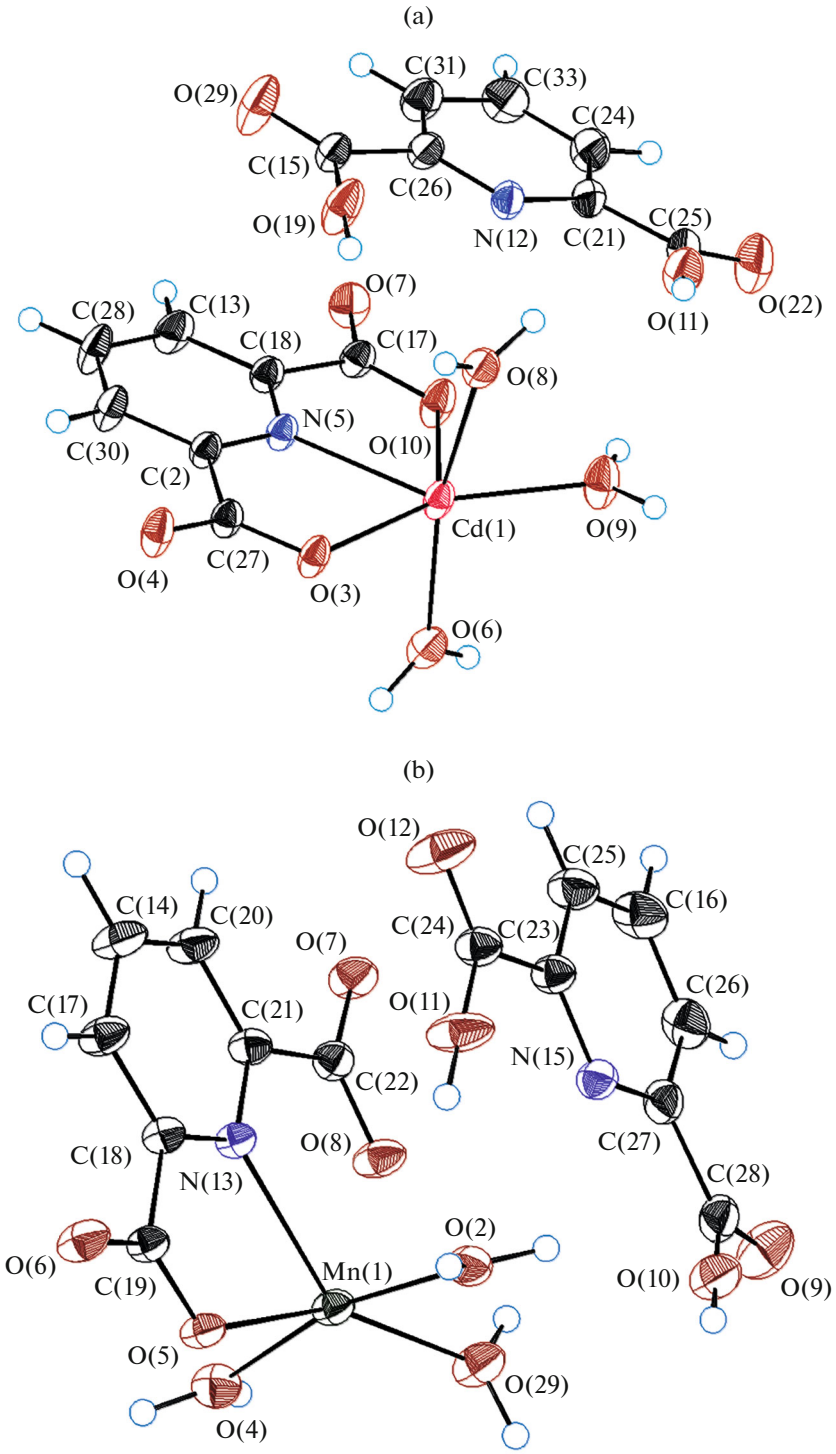

Fig. 1. An ORTEP plot of the asymmetric units of the CP **I** (a) and CP **II** (b) with atom labeling scheme.

the CPs **I** and **II**, are coincident with metallic Cd and Mn Δm% obsd. (calcd.) 22.9, 12.7% (22.5, 12.4%), respectively.

The UV-Vis absorption spectra of $PydcH_2$ and the CPs **I** and **II** reveal three absorption bands at 220–230, 245–265, and 295–315 nm, Table 5. The first two high energy bands are due to $^1L_a \leftarrow {}^1A$ and $^1L_b \leftarrow {}^1A$ transitions, respectively. These bands are shifted to lower wavelengths in the spectra of **I** and **II** than those of $PydcH_2$, confirming the coordination of the nitrogen

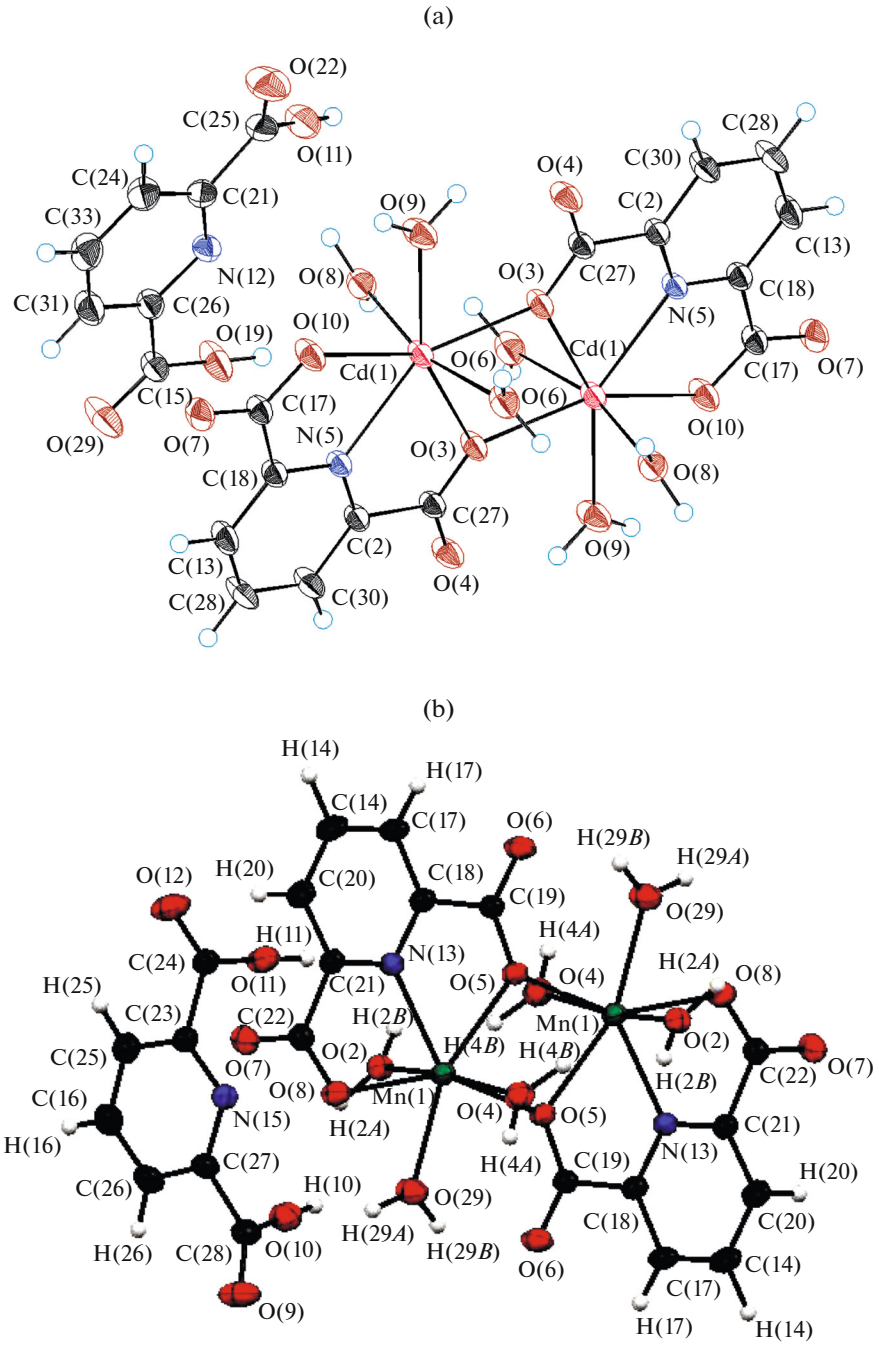

Fig. 2. The repeated units containing two asymmetric units of the CP **I** (a) and CP **II** (b).

and oxygen atoms of the ligand to metal atoms in the CPs **I** and **II**. The third band at 295–315 nm is weak corresponding to n–π* transitions (Table 5).

The solid state emission data of the CPs **I** and **II** are summarized in Table 5. It is worth mentioning that the emission spectrum of $PydcH_2$ does not show any bands in DMF solution or in solid state on excitation at 300 nm. This finding is expected as the fact that the pyridine and its derivatives are, generally, not luminescent materials [41]. On the other hand, the emission spectra of the CPs **I** and **II** reveal structured high energy and low energy bands in the visible region at 360–490 nm upon excitation at 300 nm (Table 5). The emission band at 380–420 nm for **I** and at 365, 417 nm for **II** corresponds to the lowest π–π* state in the ligand under the effect of coordination [42]. The emission bands at 490 and 485 nm in the CPs **I** and **II** are attributed to MLCT transitions.

The biological activity of the metal complexes is governed by the following factors: (i) the chelate effect

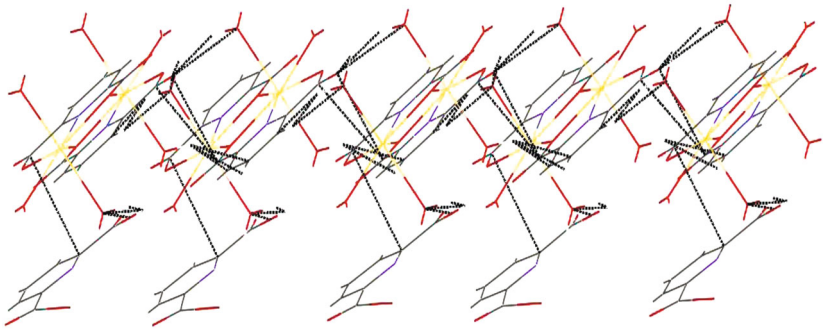

Fig. 3. 1D chain of the CP **I** via H-bonds along the *y* axis.

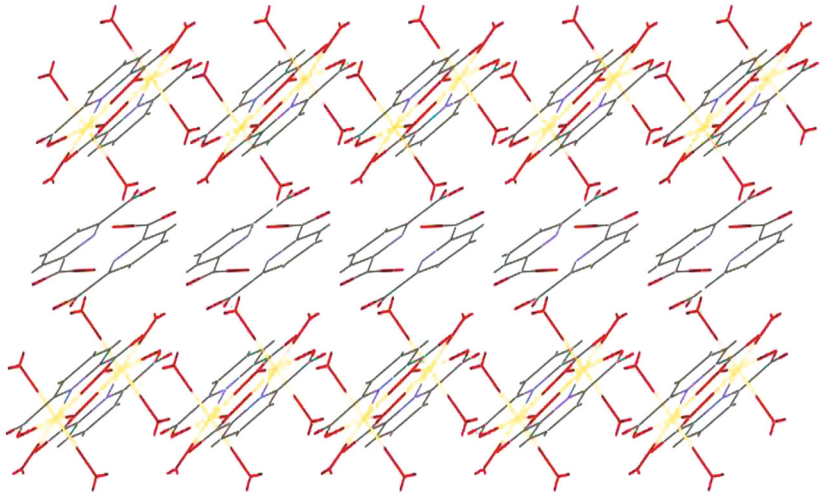

Fig. 4. 2D layer of the CP **I** via H-bonds and π–π stacking along the *y* axis.

of the ligands, (ii) the nature of the donor atoms, (iii) the total charge on the complex ion, (iv) the nature of the metal ion, (v) the nature of the counter ions that neutralize the complex, and (vi) the geometrical structure of the complex [43]. Furthermore, chelation reduces the polarity of the metal ion because of partial sharing of its positive charge with the donor groups and possibly the π-electron delocalization

Table 4. The wavenumbers (cm^{-1}) of different vibrational modes of the CP **I**, **II** and $PydcH_2$ ligand*

Compound	ν(H_2O)	ν(CH)	ν(C=O)	ν(C=N), ν(C=C)$_{ar}$	$\nu_{as}(COO^-)$, $\nu_s(COO^-)$, $\delta(COO^-)$	γ_{CH} of L	ν(M–O)	ν(M–N)	ν(COOH)
CP **I**	3250–3400 br	3084–3000 w	1693 sh	1581w	1450 w 1380 sh 697	638 w	544 w	442 w	2550 m
CP **II**	3200–3408 br	3100–3000 w	1694 sh	1593 sh	1439 s 1392 sh 655 w	726 s	542 s	441 s	2555 w
$PydcH_2$		3070 w 3004 w	1703 s 1269 m	1575 s	1575 s 1385 s 701 s	752 s			2659 m 2548 m

* br = broad, sh = sharp, m = medium, w = weak.

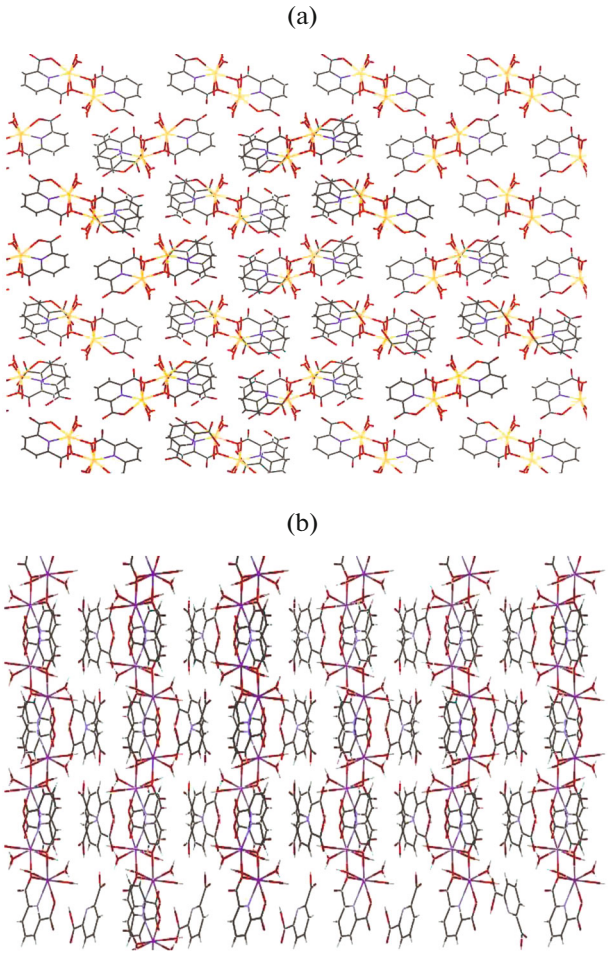

Fig. 5. 3D network of the CP **I** (a) along the *x* axis and CP **II** (b) along the *xz* axis.

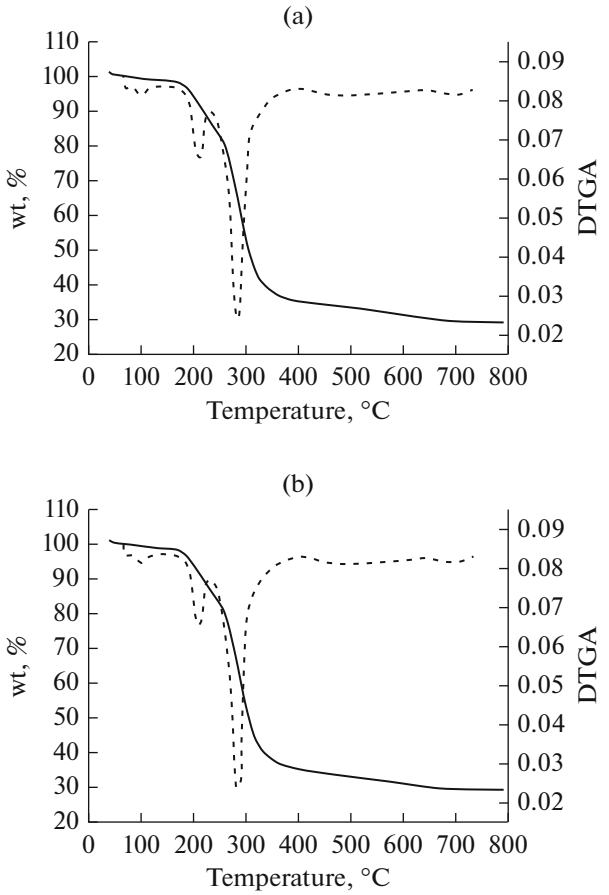

Fig. 6. Thermogravimetric analysis of CPs **I** (a) and **II** (b).

within the whole chelate ring system that is formed during coordination [44]. These factors increase the lypophilic nature of the central metal atom and hence increasing the hydrophobic character and liposolubility of the molecule favoring its permeation through the lipid layer of the bacterial membrane. This enhances the rate of uptake/entrance and thus the antibacterial activity of the testing compounds.

The CPs **I** and **II** were tested for their inhibitory effects on the growth of bacteria: *S. aureus* and *E. coli,* and fungi *A. flavus* and *C. albicans* because such organisms can achieve resistance to antibiotics through biochemical and morphological modification [45]. The antibacterial and antifungal activities of the new CPs **I** and **II** are listed in Table 6. The results indicate that the CPs **I** and **II** have antibacterial but don't have any antifungal activity on the tested microorganisms compared with the data of Ampicillin as antibacterial agent and Amphotericin B as antifungal agent. On chelation, the polarity of the metal ion will be reduced to a greater extent due to the overlap of the ligand orbital and partial sharing of the positive charge of the metal ion with donor groups. Further, it increases the delocalization of π-electrons over the whole chelate ring and enhances the penetration of the

Table 5. The electronic absorption and emission spectra of **I**, **II**

λ_{abs}, nm					λ_{em}, nm		
$PydcH_2$	assignment	**I**	**II**	assignment	**I**	**II**	assignment
230	$^1L_a \leftarrow {}^1A$	220	230	$^1L_a \leftarrow {}^1A$	380–420 br	365, 417	Close laying π–π* transitions
265	$^1L_b \leftarrow {}^1A$	245	265	$^1L_b \leftarrow {}^1A$	490	485	MLCT transitions
315	$n \rightarrow \pi^*$	295	315	$n \rightarrow \pi^*$			

Table 6. Antimicrobial and antifungal activities of the CPs **I** and **II**

Sample		Inhibition zone diameter (mm/mg sample)			
		Escherichia coli (G^-)	*Staphylococcus aureus* (G^+)	*Aspergillus flavus* (Fungus)	*Candida albicans* (Fungus)
Control: DMSO		0.0	0.0	0.0	0.0
Standard	Ampicillin Antibacterial agent	22	18		
	Amphotericin B Antifungal agent			17	19
CP **I**		15	13	0.0	0.0
CP **II**		12	11	0.0	0.0
DMSO		0.0	0.0	0.0	0.0

complexes into lipid membranes with blocking of the metal binding sites in the enzymes of microorganisms. These complexes also disturb the respiration process of the cell and thus block the synthesis of proteins, which restricts further growth of the organisms [46]. The variation in the effectiveness of different compounds against different organisms depends on either the impermeability of the cells of the microbes or on differences in ribosome of microbial cells [44].

REFERENCES

1. Yaghi, O.M., O'Keeffe, M., Ockwig, N.W., et al., *Nature*, 2003, vol. 423, p. 705.
2. Coronado, E. and Espallargas, G.M., *Chem. Soc. Rev.*, 2013, vol. 42, p. 1525.
3. Pu, L., *Acc. Chem. Res.*, 2012, vol. 45, p. 150.
4. Bodnarchuk, M.I., Erni, R., Krumeich, F., and Kovalenko, M.V., *Nano Lett.*, 2013, vol. 13, p. 1699.
5. Suh, M.P., Park, H.J., Prasad, T.K., and Lim, D.W., *Chem. Rev.*, 2012, vol. 112, p. 782.
6. Duriska, M.B., Neville, S.M., Lu, J.-Z., et al., *Angew. Chem., Int. Ed.*, 2009, vol. 48, p. 8919.
7. Lu, Z.-Z., Zhang, R., Li, Y.-Z., et al., *J. Am. Chem. Soc.*, 2011, vol. 133, p. 4172.
8. Etaiw, S.E.H. and El-Bendary, M.M., *Appl. Catal., B*, 2012, vol. 126, p. 326.
9. Etaiw, S.E.H., Sultan, A.S., and El-Bendary, M.M., *J. Organomet. Chem.*, 2011, vol. 696, p. 1668.
10. Etaiw, S.E.H. and El-Bendary, M.M., *Polyhedron*, 2015, vol. 87, p. 383.
11. Etaiw, S.E.H. and El-Bendary, M.M., *Inorg. Chim. Acta*, 2015, vol. 435, p. 167.
12. He, Y.P., Tan, Y.X., and Zhang, J., *Cryst. Growth Des.*, 2014, vol. 14, p. 3493.
13. Yang, Q.X., Chen, X.Q., Chen, Z.J.Y., et al., *Chem. Commun.*, 2012, vol. 48, p. 10016.
14. Barman, S., Khutia, A., Koitz, R., et al., *J. Mater. Chem. A*, 2014, vol. 2, p. 18823.
15. Wu, H., Yang, J., Su, Z.M., et al., *J. Am. Chem. Soc.*, 2011, vol. 133, p. 11406.
16. Hu, J.S., Huang, L.F., Yao, X.Q., et al., *Inorg. Chem.*, 2011, vol. 50, p. 2404.
17. Miao, H., Wang, Y., Cui, Y.M., and Liu, Z.D., *Z. Anorg. Allg. Chem.*, 2014, vol. 640, p. 1514.
18. Cai, Y.-P. Chen, C.-L., et al., *J. Am. Chem. Soc.*, 2003, vol. 125, p. 8595.
19. Song, X.-Z., Song, S.-Y., Qin, C., et al., *Cryst. Growth Des.*, 2012, vol. 12, p. 253.
20. Munakata, M., Wu, L.P., Kuroda-Sowa, et al., *Inorg. Chem.*, 1997, vol. 36, p. 5416.
21. Kajiwara, T. and Ito, T., *J. Chem. Soc., Dalton Trans.*, 1998, p. 3351.
22. Kamiyama, A., Noguchi, T., Kajiwara, T., and Ito, T., *Angew. Chem., Int. Ed.*, 2000, vol. 39 p, p. 3130.
23. Okabe, N. and Oya, N., *Acta Crystallogr., Sect. C: Cryst. Struct. Commun.*, 2000, vol. 56, p. 1416.
24. Odoka, M., Kusano, A., and Okabe, N., *Acta Crystallogr., Sect. E: Struct. Rep. Online*, 2002, vol. 58, p. m25.
25. French, F.A., Blanz, E.J., Amaral, J.R.D., and French, D.A., *J. Med. Chem.*, 1970, vol. 13, p. 11179.
26. Serbest, K., Özen, A., Unver, A.Y., et al., *J. Mol. Struct.*, 2009, vol. 922, p. 1.
27. Powell, J.F., *Biochem. J.*, 1953, vol. 54, p. 205.
28. Church, B.S. and Halvorson, H., *Nature*, 1959, vol. 183, p. 124.
29. Chung, L., Rajan, K.S., Merdinger, E., and Grecz, N., *Biophys. J.*, 1971, vol. 11, p. 469.
30. Drew, M.G.B., Mattews, R.W., and Walton, R.A., *J. Chem. Soc. A*, 1970, p. 1405.
31. Schwarzenbach, D., *Inorg. Chem.*, 1970, vol. 9 p, 2391.
32. Palmer, K.J., Wong, R.Y., and Lewis, J., *Acta Crystallogr., Sect. B*: *Struct. Crystallogr. Cryst. Chem.*, 1972, vol. 28, p. 223.
33. Quaglieri, P.P., Loiseleur, H., and Thomas, G., *Acta Crystallogr., Sect. B*: *Struct. Crystallogr. Cryst. Chem.*, 1972, vol. 28, p. 2583.
34. Laine, Â.P., Gourdon, A., and Launay, J.-P., *Inorg. Chem.*, 1995, vol. 34, p. 5129.
35. Okabe, N. and Oya, N., *Acta Crystallogr., Sect. C: Cryst. Struct. Commun.*, 2000, vol. 56, p. 305.

36. Laine, Â.P., Strahs, A.G., and Dickerson, R.E., *Acta Crystallogr., Sect. B*: *Struct. Crystallogr. Cryst. Chem.*, 1968, vol. 24, p. 571.

37. Gourdon, A., Launay, J.-P., and Tuchagues, J.-P., *Inorg. Chem.*, 1995, vol. 34, p. 5150.

38. Aghabozorg, H., Sadr-Khanlou, E., Shokrollahi, A., et al., *J. Iran. Chem. Soc.*, 2009, vol. 6, p. 55.

39. Aghajani, Z., Aghabozorg, H., Sadr-Khanlou, E., et al., *J. Iran. Chem. Soc.*, 2009, vol. 6, p. 373.

40. Deacon, G.B. and Philips, R.J., *Coord. Chem. Rev.*, 1980, vol. 33, p. 227.

41. Valeur, B., *Molecular Fluorescence Principles and Applications*, Weinheim: Wiley-VCH, 2002, p. 59.

42. Jaffé, H.H. and Orchin, M., *Theory and Applications of Ultraviolet Spectroscopy*, Wiley, 1970.

43. Efthimiadou, E.K., Psomas, G., Sanakis, et al., *J. Inorg. Biochem.*, 2007, vol. 101, p. 525.

44. Lawrence, P.G., Harold, P.L., and Francis, O.G., *Antibiot. Chemother.*, 1980, vol. 5, p. 1597.

45. Mandal, S.K. and Nag, K., *J. Chem. Soc., Dalton Trans.*, 1983, vol. 11, p. 2429.

46. Dharmaraj, N., Viswanathamurthi, P., and Natarajan, K., *Transition Met. Chem.*, 2001, vol. 26, p. 105.